Vol 10 No 1, January 2001
1009-1963/2001/10(01)/0058-07

Chinese Physics

©2001 Chin. Phys. Soc.
and IOP Publishing Ltd

FLUORESCENCE MECHANISMS OF Tm^{3+}- AND Yb^{3+}/Tm^{3+} DOPED AlF_3-BASED FLUORIDE GLASS

Zhang Long(张 龙), Zhang Jun-jie(张军杰), Hu He-fang(胡和方), and Lin Feng-ying(林凤英)
Shanghai Institute of Optics and Fine Mechanics, Chinese Academy of Sciences, Shanghai 201800, *China*

(Received 23 March 2000; revised manuscript received 21 August 2000)

A complete set of spectroscopic parameters, including Judd-Ofelt parameters, radiative transition probabilities, radiative lifetime, branching ratios and integrated absorption cross section, have been calculated for Tm^{3+}- doped fluoroaluminate (AYF) glass, based on the measured absorption spectra. The mechanism of $Tm^{3+} \rightarrow Tm^{3+}$ and $Yb^{3+} \Leftrightarrow Tm^{3+}$ energy transfers and fluorescence properties have been investigated in both Tm^{3+} single-doped and Yb^{3+}/Tm^{3+} double-doped AYF glasses. The cross-relaxation process, $^3F_4+{}^3H_6 \rightarrow 2{}^3H_4$, is proved, which makes the optimum Tm^{3+} concentration of 1.77μm fluorescence ($^3H_4 \rightarrow {}^3H_6$) much higher than 1.45$\mu$m fluorescence ($^3F_4 \rightarrow {}^3H_4$) in Tm^{3+}:AYF glasses. In Yb^{3+}/Tm^{3+}:AYF glasses, a stronger concentration quenching is found for the 476nm emission than that for the 797nm emission, and is discussed under the 970nm-excitation.

Keywords: fluoroaluminate glass, Judd-Ofelt analysis, energy transfer, rare earth
PACC: 7855, 4255R, 7840

I. INTRODUCTION

Glasses doped with Tm^{3+} ion have been investigated as potential hosts of visible and near infrared laser because of the attractive transitions of Tm^{3+} ion in visual and infrared regions: The transition $^1G_4 \rightarrow {}^3H_6$ (~480nm) is in blue region. The transition $^3F_4 \rightarrow {}^3H_4$ (~1.45μm) can be applied as a useful source for water or humidity sensing.[1] A high-power 1.45μm Tm^{3+}-doped fiber laser is promising as the pump source for a high output power Er^{3+}-doped fiber laser amplifier.[2] The transition $^3H_4 \rightarrow {}^3H_6$(~2$\mu$m) is in eye-safe region and expected to find a number of application in eye-safe lidar, remote sensing of glasses and medical field.[3]

Fluoride glasses are attractive host material for rare earth (RE) laser and amplifiers because they have a lower phonon energy than oxide glasses. Zr_4-based (fluorozirconate) and AlF_3-based (fluoroaluminate) glasses are two main types of fluoride glasses. Recently, a considerable number of papers have been published on the upconversion and near-infrared emissions from Tm^{3+} and Yb^{3+}/Tm^{3+} doped ZrF_4-based glasses, such as ZBLAN.[1–7] However, there has been less discussion of the AlF_3-based glasses doped with Tm^{3+} and Yb^{3+}/Tm^{3+}. Quite recently, we systematically investigated AlF_3-based glasses doped with Er^{3+}, Yb^{3+}/Er^{3+}, Tm^{3+}, and Yb^{3+}/Tm^{3+} ions. Experimental results have shown that AlF_3-based glasses might be a better option for optical component.[8] The purpose of this paper is to investigate the fluorescence mechanisms of Tm^{3+} and Yb^{3+}/Tm^{3+} doped AlF_3-based glasses with a laser diode (LD) at 800 and 970nm. A Judd-Ofelt analysis has been employed to determine the radiative transition probability (A), lifetimes (τ_R), branching-ratios (β) and integrated absorption cross-section (σ_a) for Tm^{3+} transitions in AlF_3-based glasses.

II. EXPERIMENTAL PROCEDURE

Glasses with the composition of 35AlF_3- (15-x-y) YF_3-50RF_2-$x$$TmF_3$-$y$$YbF_3$ (R=Mg, Ca, Sr, and Ba) were prepared by using reagent pure $(NH_4)_3AlF_6$, YF_3, MgF_3, CaF_2, SrF_2, BaF_2, TmF_3 and YbF_3. A small mount of NH_4HF_2 was also added to complete the fluorination. The mixture of powders was melt in Pt crucible at 900–1000°C for 30min. The melt was cast into an aluminum mold. The obtained glass samples were cut and polished with a size of 20mm×15mm×3mm.

Room-temperature absorption spectra of samples were recorded using a double-beam spectrophotometer (Perkin-Elmer Lambda 9). The fluorescence spectra were obtained by exciting the samples with light from a diode laser operating at 800 and 970nm.

The index of refraction was measured at two wavelengths and the indices of refraction at all other wavelengths were calculated using Cauchy's equation $n = A + B/\lambda^2$, where A=1.4326 and B=3610.17nm^2

were obtained in our samples.

Ⅲ. EXPERIMENTAL RESULT

A. Physical and chemical properties of AYF glass

The chemical durability of the AYF and ZBLAN glasses was measured on the basis of the surface weight loss of the bulk samples after immersion in distilled water at a constant temperature for several hours. The results are given in Fig.1. Table 1 presents other physical properties of the glasses determined by conventional methods. It can be seen that AYF glass has a higher glass transition temperature (T_g) and is more chemically and mechanically durable than ZBLAN glass.

Table 1. Physical properties of fluoride glasses.

Property	AYF	ZBLAN
Transition region/μm	0.23−7.0	0.24−7.5
Density/(g/cm^3)	3.87	4.62
Abbe's value ν_d	97	76
Transition temperature T_g	438	315
Softening temperature T_f	425	300
Young's modulus/(10^5kg/cm^2)	7.16	5.53
Thermal expansion/10^{-7}°C^{-1}	149	157

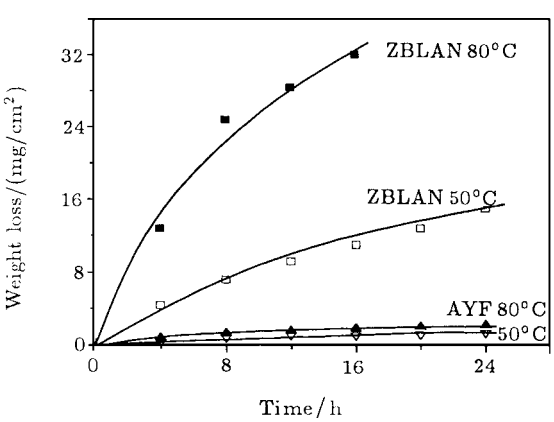


Fig.1. Weight loss of fluoride glasses as a function of the immersion time in distilled water at a constant temperature.

B. Oscillator strengths and Judd-Ofelt analysis of Tm^{3+}

The room-temperature absorption spectrum for Tm^{3+}-doped (2mol%) AYF glass is shown in Fig.2. The energy levels of Tm^{3+} ion in AYF glasses assigned from this spectrum are also shown in Fig.2.

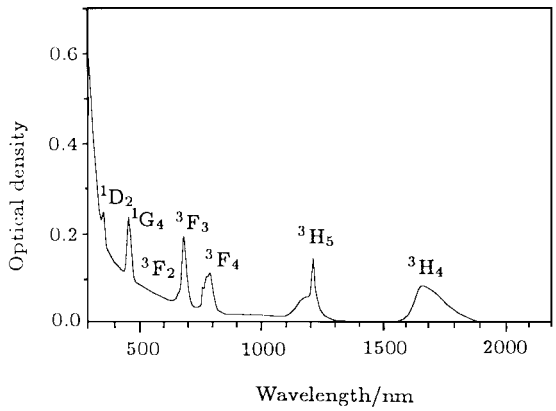


Fig.2. Absorption spectrum of Tm^{3+} in AYF glass.

The oscillator strengths are determined experimentally using the following equation:

$$P_{\exp}(J, J') = \frac{mc^2}{N\pi e^2} \int k \mathrm{d}\nu, \qquad (1)$$

$$k = 2303E/d,$$

where c is the speed of light, N the number of active ions per unit volume, E the absorbance and d the sample thickness. The parameters m and e are the electron mass and charge (in electrostatic units), respectively. The experimental oscillator strengths for Tm^{3+}:AYF glass are presented in Table 2.

The theoretical oscillator strength is calculated by use of the J-O theory.[9,10] For the electric dipole transition $SLJ \rightarrow S'L'J'$ of frequency ν, the calculated oscillator is

$$P_{\mathrm{calc}}(J; J') = \frac{8\pi^2 m\nu}{3h(2J+1)} \frac{(n^2+2)^2}{9n} \cdot \sum_{t=2,4,6} \Omega_t (\langle SLJ \parallel U^{(t)} \parallel S'L'J' \rangle)^2, \qquad (2)$$

where $n(\lambda)$ is the refractive index of the medium as a function of wavelength, $\Omega_t (t = 2, 4, \text{ and } 6)$ are three J-O intensity parameters, $U^{(t)}$ is the double-reduced matrix element of the unit tensors, which are taken from Ref.[11] since they are almost insensitive to the ion environment. All transitions are assumed to be electric dipolar in nature, except the $^3H_6 \rightarrow {}^3H_5$ transition which exhibits a non-negligible magnetic dipolar contribution.

Table 2. Oscillator strengths of Tm^{3+} ions in AYF glass.

Transitions	λ/nm	$P_{exp}/10^{-8}$	$P_{calc}/10^{-8}$	Residuals/10^{-8}
$^3H_6 \rightarrow {}^3H_4$	1680	161	169	−8
$^3H_5$	1203	130	125	+5
$^3F_4$	780	185	175	+10
$^3F_3$	681	289	243	−3
$^3F_2$	658		49	
$^1G_4$	461.6	63	51	+12

The three J-O parameters Ω_t are determined by fitting the five experimentally obtained oscillator strengths using Eq.(2) by the least-squares analysis:

$$\Omega_2 = 1.77 \times 10^{-20}\mathrm{cm}^2,$$

$$\Omega_4 = 1.58 \times 10^{-20}\mathrm{cm}^2,$$

$$\Omega_6 = 1.16 \times 10^{-20}\mathrm{cm}^2.$$

The quality of the fit is given by the root-mean-square deviation which is equal to 13×10^{-8}.

The oscillator strengths for Tm^{3+} transitions calculated using these Ω_t values are also given in Table 2. A reasonable agreement between the measured and calculated oscillator strengths has been obtained.

The spontaneous emission probability $A(J; J')$ for the electric-dipole emission can be estimated using the following expression:

$$A(J; J') = \frac{64\pi^4 e^2}{3h(2J+1)\lambda^2} \frac{n(n^2+2)^2}{9n} \cdot \sum_{t=2,4,6} \Omega_t (\langle SLJ \parallel U^{(t)} \parallel S'L'J' \rangle)^2. \quad (3)$$

The emission branching ratio of a transition is defined as

$$\beta(J; J') = A(J; J') / \sum_{J'} A(J; J'). \quad (4)$$

For laser analysis of rare earth material the integrated absorption cross-section, σ_a, for stimulator emission is estimated from

$$\sigma_a = \frac{\lambda^2}{8\pi c n^2} A. \quad (5)$$

The calculated values of A, τ_R, β, and σ_a for various luminescent transitions are given in Table 3.

Table 3. Predicted radiative transition probabilities (A) ,total radiative transition probabilities (A_T), radiative lifetime (σ_R), branching ratios (β),integrated absorption cross-section for stimulated emission (σ_a), for certain selected excited levels of Tm^{3+} in AYF glasses. Wavelengths are determined from emission spectra when possible.

Transition	Wavelength/nm	A/s^{-1}	A_T/s^{-1}	τ_R/ms	$\sigma_a/10^{-18}$cm	β_i
$^3H_4 \rightarrow {}^3H_6$	1770	110.2	110.2	9.07	2.228	1
$^3F_4 \rightarrow {}^3H_6$	797	536.7			2.186	0.83
$^3H_4$	1450	97.6	646.7	1.54	1.323	0.15
$^3H_5$	2280	12.4			0.416	0.02
$^1G_4 \rightarrow {}^3H_6$	476	462.4			0.662	0.43
$^3H_4$	651	82.5			0.223	0.08
$^3H_5$	778	381.6	1080.5	0.93	1.481	0.35
$^3F_4$	1181	111.0			1.505	0.10
$^3F_3$	1531	33.6			0.508	0.03
$^3F_2$	1678	9.4			0.171	0.01

C. Infrared emission properties of Tm^{3+} in AYF glasses

Under LD excitation at 800nm, the infrared fluorescence emissions around 1.45μm ($^3F_4 \rightarrow {}^3H_4$) and 1.77$\mu$m ($^3H_4 \rightarrow {}^3H_6$) were observed in Tm^{3+}:AYF

glasses. As shown in Table 3, both transitions have large branching ratios. For an understanding of concentration dependence of the fluorescence, we measured the fluorescence intensities of various Tm^{3+} concentrations. The results are shown in Fig.3. The maximum intensity of the 1.45μm-emission was observed in the range of 0.2–0.5mol% TmF_3. In contrast, the fluorescence quenching of the 1.77μm emission was not observed until 2mol% TmF_3. This behavior may be due to the cross relaxation, $^3F_4+{}^3H_6 \rightarrow 2{}^3H_4$, as shown in Fig.4.

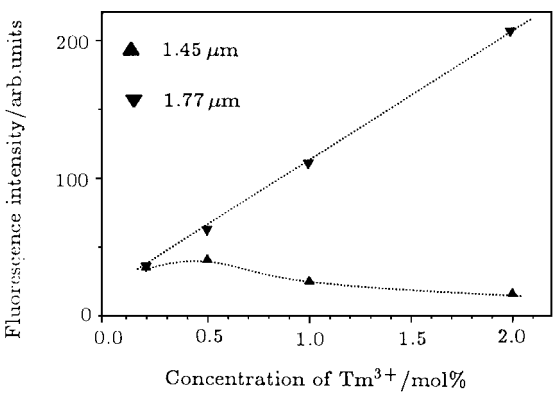


Fig.3. Relationship between the fluorescent intensities of $^3H_4 \rightarrow {}^3H_6$(1.77$\mu$m)and $^3F_4 \rightarrow {}^3H_4$(1.45$\mu$m), and Tm^{3+} concentration in AYF glasses.

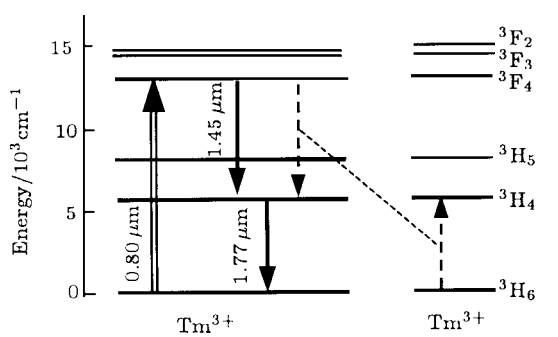


Fig.4. Energy-level diagram of Tm^{3+} ions, showing infrared emission and the cross-relaxation process.

The probability of this energy transfer is proportional to R^{-6},[12] where R is distance between neighboring ions. With the increase of the Tm^{3+} concentration, the value of R decreases, which causes the quantum efficiency of $^3F_4+{}^3H_6 \rightarrow 2{}^3H_4$ energy transfer to increase. As a result, concentration quenching of fluorescence intensity will shift to a lower Tm^{3+} concentration for the $^3F_4 \rightarrow {}^3H_4$ transition, and in contrast, to a higher Tm^{3+} concentration for the $^3H_4 \rightarrow {}^3H_6$ transition. In other words, the maximum intensity of the $^3H_4 \rightarrow {}^3H_6$ fluorescence will occur at a higher Tm^{3+} concentration after the cross relaxation of $^3F_4+{}^3H_6 \rightarrow 2{}^3H_4$ is saturated at a certain Tm^{3+} concentration, and in contrast, the $^3F_4 \rightarrow {}^3H_4$ fluorescence will occur at a lower Tm^{3+} concentration.

D. Upconversion fluorescence properties in Yb^{3+}/Tm^{3+} co-doped AYF glasses

Under a 970nm LD excitation at room temperature, the strong upconversion fluorescence centered at 476 and 797nm were observed in Yb^{3+}/Tm^{3+}:AYF glasses, which correspond to the $^3F_4 \rightarrow {}^3H_6$ and $^1G_4 \rightarrow {}^3H_6$ transitions, respectively. The dependence of the emission intensity on the excitation power (P_{ex}) is plotted in Fig.5. The slopes of the 476 and 797nm emissions are 2.56 and 1.85, respectively. These dependences indicate that the $^1G_4$ and $^3F_4$ levels are populated mainly through the three- and two-photon processes, respectively.

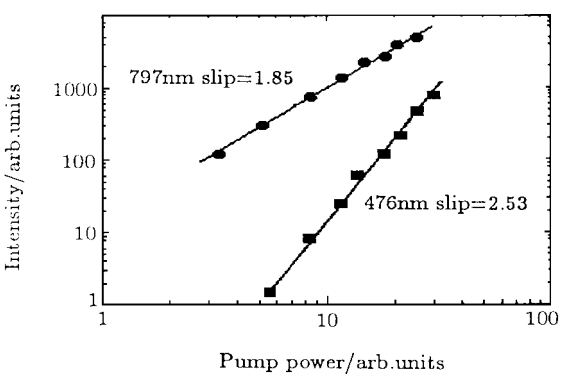


Fig.5. The log-log plot of the fluorescence intensity versus pump power. The contents of YbF_3 and TmF_3 are 5 and 0.2mol%, respectively.

In order to examine the characteristics of the 476 and 797nm upconversion fluorescence, the dependences of both fluorescences upon the concentrations of Tm^{3+} and Yb^{3+} were measured, as shown in Figs.6 and 7. It can be seen that both fluorescence intensities first increase and then decrease with increasing concentration of Tm^{3+} and Yb^{3+}. The maximum intensities of the fluorescences occur at a higher concentration for Yb^{3+} ions than for Tm^{3+} ions. As shown in Fig.6, the maximum fluorescence intensity is observed approximately at 0.1mol% Tm^{3+} for the 476nm fluorescence, while it is about 0.5mol% for the 797nm fluorescence. Therefore, compared with the 797nm emission, the concentration quenching of the 476nm blue emission is more apparent. From Fig.7, we can observe that for both emissions, the optimum Yb^{3+} concentrations are around 5mol%.

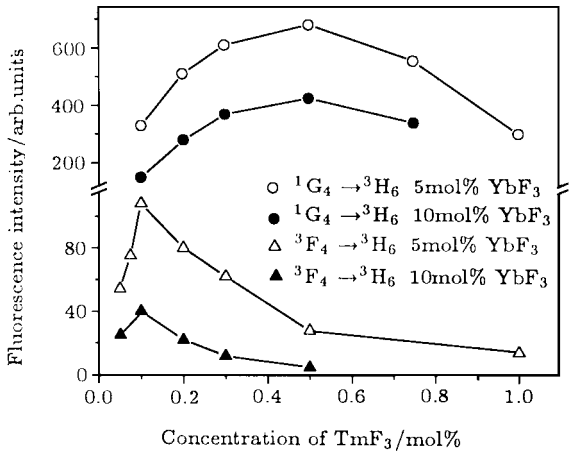


Fig.6. Concentration dependence of the fluorescence intensity on Tm^{3+} in Yb^{3+}/Tm^{3+} co-doped AYF glass, excited at 970nm.

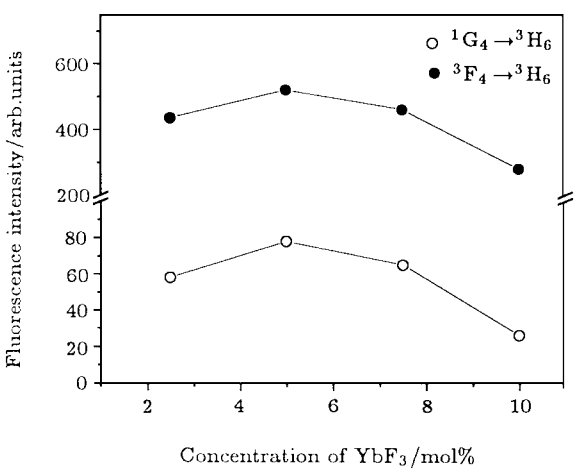


Fig.7. Concentration dependence of the fluorescence intensity on Yb^{3+} in Tm^{3+}(=0.2mol%), Yb^{3+} co-doped AYF glass, excited at 970nm.

IV. DISCUSSION

In this section, we discuss the upconversion mechanisms and energy transfer in Yb^{3+}/Tm^{3+} co-doped AYF glass system. The essential feature for the upconversion emission under infrared pumping can be obtained by considering the energy level diagrams for Yb^{3+} and Tm^{3+} in Fig.8. Under the excitation of 970nm, the Yb^{3+} ion was first excited to the $^2F_{5/2}$ level, and then after a multi-step energy transfer process Tm^{3+} ion was excited to the levels of $^3F_4$, $^1G_4$. The energy transfer process may be assisted by phonons (PET). This mechanism can be expressed as follows:[13]

$$\mathrm{ET1}: Yb^{3+}(^2F_{5/2})+Tm^{3+}(^3H_6) \rightarrow Yb^{3+}(^2F_{7/2}) + Tm^{3+}(^3H_5) + \text{phonons}, \quad (6)$$

$$Tm^{3+}(^3H_5) \rightarrow Tm^{3+}(^3H_4), \quad (7)$$

$$\mathrm{ET2}: Yb^{3+}(^2F_{5/2})+Tm^{3+}(^3H_4) \rightarrow Yb^{3+}(^2F_{7/2}) + Tm^{3+}(^3F_2) + \text{phonons}, \quad (8)$$

$$Tm^{3+}(^3F_2, ^3F_3) \rightarrow Tm^{3+}(^3F_4), \quad (9)$$

$$\mathrm{ET3}: Yb^{3+}(^2F_{5/2})+Tm^{3+}(^3F_4) \rightarrow Yb^{3+}(^2F_{7/2}) + Tm^{3+}(^1G_4) + \text{phonons}. \quad (10)$$

Equations 7 and 9 show the multiphonon nonradiative relaxation processes. The above equations (6)–(10) show that the 476nm emission is a three-photon process, and that the 797nm emission is a two-photon process. This is verified by the relationship of the emission intensity with the excitation power shown in Fig.5.

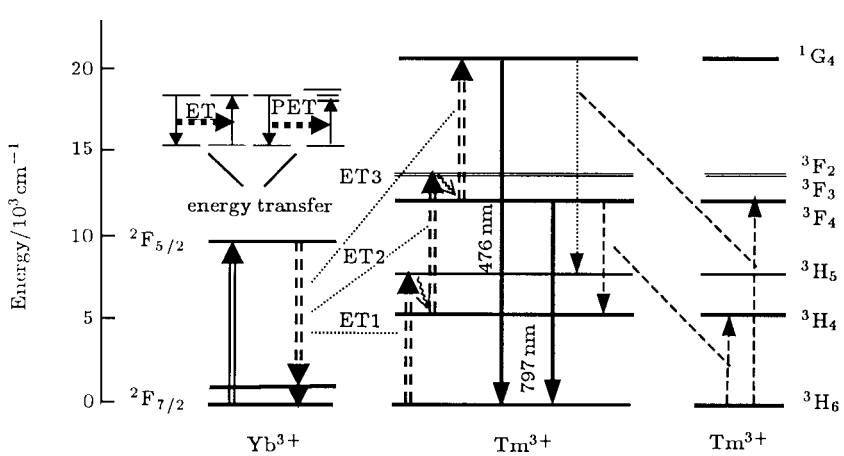


Fig.8. The absorption and energy level diagram of Tm^{3+} and Yb^{3+}, the upconversion excitation scheme and the cross-relaxation process in AYF glass. The solid arrows represent the radiative phenomena, the dashed arrows represent the Yb-Tm energy transfer process.

Under dipole-dipole interaction, the probability of the energy transfer process, P, can be expressed as:[12]

$$P = \text{constant} \times (\Pi \times S)/R^6, \qquad (11)$$

where Π is determined by the product of the electric dipole probabilities of the two transitions, S is an overlap integral (which is mainly determined by the energy mismatch (ΔE) between the two transitions in the energy transfer process), R is the distance between Yb^{3+} and Tm^{3+} ions. In AYF glass the Yb^{3+} ions can be doped with a high concentration without devitrificaton and RE clustering, so that the distance, R, is small. The ΔE values of the above ET process are calculated from Tables 2 and 3, and are listed in Table 4. It can be seen that the ΔE values of ET1, ET2, and ET3 are small.

Table 4. Energy mismatches ΔE of upconversion energy transfer and cross relaxation.

Upconversion energy transfer	$\Delta E/cm^{-1}$	Cross relaxation	$\Delta E/cm^{-1}$
ET1:$Yb(^2F_{5/2})+Tm(^3H_6)\rightarrow Yb(^2F_{7/2})+Tm(^3H_5)$	1787	$^1G_4+^3H_6\rightarrow{}^3H_4+{}^3F_2$	149
ET2: $Yb(^2F_{5/2})+Tm(^3H_4)\rightarrow Yb(^2F_{7/2})+Tm(^3F_2)$	755	$^1G_4+^3H_6\rightarrow{}^3H_4+{}^3F_3$	654
ET3: $Yb(^2F_{5/2})+Tm(^3F_4)\rightarrow Yb(^2F_{7/2})+Tm(^1G_4)$	1129	$^1G_4+^3H_6\rightarrow{}^3H_5+{}^3F_4$	155
*ET4:$Tm(^3F_4)+Yb(^2F_{7/2})\rightarrow Tm(^3H_6)+Yb(^2F_{5/2})$	2610	$^3F_4+^3H_6\rightarrow 2^3H_4$	944

*Back-energy transfer from $Tm^{3+}\rightarrow Yb^{3+}$.

Furthermore, the energy levels of RE ions extend widely in glass, especially in fluoride glass with a great disorder in the RE environment,[14] which results in a spectral overlap between the Yb^{3+} emission ($^2F_{5/2}\rightarrow{}^2F_{7/2}$) and Tm^{3+} absorption. For instance, the band (9451–11628cm^{-1}) of the Yb^{3+} emission ($^2F_{5/2}\rightarrow{}^2F_{7/2}$) actually overlaps partially with the band (7233–10827cm^{-1}) of the Tm^{3+} absorption ($^3H_6\rightarrow{}^3H_5$) in the ET2 process. Therefore, due to the partial overlap, the ΔE values are in fact less than those given in Table 4.

In addition, the small lifetimes of the $^3H_5$ and $^3F_{2,3}$ levels make the back-energy transfer from Tm^{3+} to Yb^{3+} hard to carry out. For these reasons, the energy transfer efficiencies of ET1, ET2 and ET3 processes are large in AYF glass, so that the strong upconversion fluorescences around 476 and 797nm can be observed in Yb^{3+}/Tm^{3+}:AYF glass with the 970nm-excitation.

Several expressions have been derived for both upconversion fluorescence intensities using rate equation models. The upconversion fluorescence intensities for the $^3F_4\rightarrow{}^3H_6$ (I_1) and $^1G_4\rightarrow{}^3H_6$ (I_2) transitions of the Yb^{3+}/Tm^{3+} system, using the same approach reported by Wright,[15] are given by

$$I_1 \propto \phi^2 {N_{Yb}}^2 N_{Tm}, \qquad (12)$$

$$I_2 \propto \phi^3 {N_{Yb}}^3 N_{Tm}, \qquad (13)$$

where N_{Yb} and N_{Tm} are concentrations of Yb^{3+} and Tm^{3+}, respectively, and ϕ is the incident pumping flux. In these expressions, the output intensities, I_1 and I_2, respectively, depend quadratically and cubically upon the incident pumping flux (ϕ). The dependences indicate that the upconversion processes for the $^3F_4\rightarrow{}^3H_6$ and $^1G_4\rightarrow{}^3H_6$ transitions are two- and three-photon processes, respectively, in the Yb^{3+}/Tm^{3+} system under the 970nm-excitation. In addition, according to Eqs.(12) and (13), the fluorescence intensities, I_1 and I_2, respectively, depend quadratically and cubically upon the concentrations of Yb^{3+} ions, and linearly upon the concentration of Tm^{3+} ions. However, the dependences are not found, as shown in Figs.6 and 7.

When increasing Tm^{3+} concentration with constants of ϕ and N_{Yb}, the 476 and 797nm emission intensities become lower for higher Tm^{3+} concentration, due to the fluorescence quenching by the cross-relaxation process between Tm^{3+} ions. Several possible cross-relaxation processes of Tm^{3+} ion and their ΔE are listed in Table 4. Each item in the table includes two processes, such as $^1G_4+^3H_6\rightarrow{}^3H_5+{}^3F_4$ including ($^1G_4\rightarrow{}^3H_5$, $^3H_6\rightarrow{}^3F_4$) and ($^1G_4\rightarrow{}^3F_4$, $^3H_6\rightarrow{}^3H_5$) processes. As shown in Table 4, these cross-relaxation processes, which are related to the $^1G_4$ and $^3F_4$ levels, have small ΔE, causing a large probability of cross relaxation. With an increasing Tm^{3+} concentration, these cross-relaxation processes will become more significant according to Eq.(11), which will decrease the population in the $^1G_4$ and $^3F_4$ levels. From Table 4, we can find that the $^1G_4$ level has a larger number of cross-relaxation processes and smaller ΔE values than the $^3F_4$ level. Furthermore, the cross relaxation processes related to the $^3F_4$ level also affect the population in the $^1G_4$ level, accord-

ing to Eq.(10). Therefore, the effect of concentration quenching is more apparent for the 476nm emission ($^1G_4 \rightarrow {}^3H_6$) than for the 797nm-emission ($^3F_4 \rightarrow {}^3H_6$).

When increasing the donor Yb^{3+} concentration with constants of ϕ and N_{Tm}, both 476 and 797nm fluorescence intensities increase at the beginning due to the increase of the donor concentration. The maximum intensities of both fluorescences are observed around 5mol%. The subsequent decrease may be due to the back-energy transfer, $^3F_4$ (Tm^{3+})$\rightarrow {}^2F_{5/2}$ (Yb^{3+}). The higher the Yb^{3+} concentration, the larger the probability of this back-energy transfer. Figure 9 shows the evidence of the back-energy transfer; when the Yb^{3+} concentration becomes higher, the fluorescence lifetime of the $^3F_4$ level decreases. Therefore, the higher concentration of Yb^{3+} will decrease

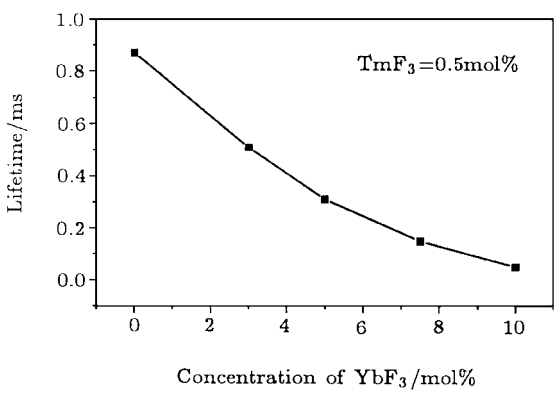


Fig.9. The linftime $^3F_4$ of level vs concentration of and Yb^{3+} in AYF glass.

the population in $^3F_4$ and $^1G_4$ levels (through ET3 process as in Eq.(10)), and quench the fluorescences of $^3F_4 \rightarrow {}^3H_6$ and $^1G_4 \rightarrow {}^3H_6$ emissions.

V. CONCLUSION

AYF glass has a higher glass transition temperature (T_g) and is chemically and mechanically more durable than ZBLAN glass.

The infrared fluorescence corresponding to the $^3F_4 \rightarrow {}^3H_4$ and $^3H_4 \rightarrow {}^3H_6$ transitions was observed in Tm^{3+}-doped AYF glass upon 800nm LD excitation. The optimum Tm^{3+} concentration of 1.77μm fluorescence ($^3H_4 \rightarrow {}^3H_6$) is much higher than that of 1.45μm fluorescence ($^3F_4 \rightarrow {}^3H_4$). It is mainly due to the cross-relaxation process, $^3F_4 + {}^3H_6 \rightarrow 2{}^3H_4$.

Under 970nm LD excitation, the strong upconversion fluorescences around 797nm ($^3F_4 \rightarrow {}^3H_6$) and 476nm ($^1G_4 \rightarrow {}^3H_6$) are observed in Yb^{3+}/Tm^{3+} co-doped AYF glass. The concentration quenching for the 476nm emission is stronger than that of the 797nm emission: the optimum Tm^{3+} concentration for the 476nm emission is about 0.1mol%, while it is in the range of 0.3–0.5mol% for the 797nm-emission.

In this paper we have presented a complete picture of the calculated spectroscopic parameters, such as the *J-O* parameters, radiative transition probabilities, radiative lifetimes, branching ratios and absorption of Tm^{3+} ions in AYF glasses, which are highly useful for analysis.

REFERENCES

[1] Mcaleavey F J, Macraith B D 1995 *Electron Lett.* **31** 1379

[2] Miyajima Y, Komukai T, Sugawe T 1993 *Electron Lett.* **29** 660

[3] Hanna D C, Perry I R, Lincoln J R 1990 *Opt. Commun.* **80** 52

[4] Le Flohic M P, Allain J Y, Stephan G M, Maze G 1994 *Opt. Lett.* **19** 1982

[5] Sanz J, Cases R, Alcala R 1987 *J. Non-Cryst. Sol.* **93** 377

[6] Feng Y, Chen X B, Hao Z *et al* 1997 *Acta Physica Sinica* **46** 2454(in Chinese)

[7] Chen X B, Zhang G Y, Li M X *et al* 1999 *Acta Physica Sinica* (*Overseas Edition*) **8** 216

[8] Zhang L, Hu H F, Lin F Y *Mater. Lett.* to be published

[9] Judd B R 1962 *Phys. Rev.* **127** 750

[10] Ofelt G S 1962 *J. Chem. Phys.* **37** 511

[11] Spector N, Reisfeld R, Boehm L 1977 *Chem. Phys. Lett.* **49** 49

[12] Kushida T 1973 *J. Phys. Soc. Jpn.* **34** 1318

[13] Auzel F E 1973 *Proc. IEEE* **61** 758

[14] Eters P M, Houde-Walter S N 1998 *J. Non-Cryst. Sol.* **239** 162

[15] Wright J C 1976 *Top. Appl. Phys.* **15** 239